ELSEVIER

Biochimica et Biophysica Acta 1369 (1998) 109–118

BIOCHIMICA ET BIOPHYSICA ACTA
BBA

Structure of yeast plasma membrane H^+-ATPase: comparison of activated and basal-level enzyme forms

Fabio Tanfani [a], Georgios Lapathitis [b], Enrico Bertoli [a], Arnošt Kotyk [b,*]

[a] *Institute of Biochemistry, Medical School, University of Ancona, Via Ranieri, 60131 Ancona, Italy*
[b] *Institute of Physiology, Academy of Sciences of the Czech Republic, Vídeňská 1083, 142 20 Prague 4, Czech Republic*

Received 21 August 1997; accepted 4 September 1997

Abstract

Plasma membrane H^+-ATPase of the yeast *Saccharomyces cerevisiae* was isolated and purified in its two forms, the activated A-ATPase from glucose-metabolising cells, and the basal-level B-ATPase from cells with endogenous metabolism only. Structure of the two enzyme forms and the effects of β,γ-imidoadenosine 5′-triphosphate (AMP-PNP) and of diethylstilbestrol (DES) thereon were analysed by FT-IR spectroscopy. IR spectra revealed the presence of two populations of α-helices with different exposure to the solvent in both the A-ATPase and the B-ATPase. AMP-PNP did not affect the secondary structure of A-ATPase while DES affected the ratio of the two α-helix populations. Thermal denaturation experiments suggested a more stable structure in the B-form than in the A-form. AMP-PNP stabilised the A-ATPase structure while DES destabilised both enzyme forms. IR spectra showed that 60% of the amide hydrogens were exchanged for deuterium in both forms at 20°C. The remaining 40% were exchanged at higher temperatures. The maximum amount of H/D exchange was observed at 50–55°C for both enzyme forms, while in the presence of DES it was observed at lower temperatures. The data do not contradict the possibility that the activation of H^+-ATPase is due to the C-terminus of the enzyme dissociating from the ATP-binding site which is covered by it in the less active form. © 1998 Elsevier Science B.V.

Keywords: Yeast plasma membrane; H^+-ATPase; Secondary structure; Fourier transform-infrared (FT-IR) spectroscopy

1. Introduction

The plasma membrane proton-translocating adenosinetriphosphatase (hereafter, H^+-ATPase) is a P-type ATPase which, during its reaction cycle, is covalently phosphorylated at an aspartate residue (number 378 in *Saccharomyces cerevisiae PMA1*-coded enzyme). It occurs as a single polypeptide chain crossing the membrane, probably ten times, with both the N- and C-termini located intracellularly, its molar mass being almost exactly 100 kDa. In yeast membranes it is accompanied by three small proteolipids which may influence the activity of the ATPase proper. (For more detailed information see, e.g. Refs. [1–6].)

The enzyme molecule contains several functional domains, starting at the N-terminus with the phosphatase domain, the phosphorylation domain, the ATP-binding and kinase domain and the C-terminal regulatory domain (e.g. Ref. [7]), the last-named be-

Abbreviations: A-ATPase, metabolically activated H^+-ATPase; B-ATPase, basal-level H^+-ATPase; AMP-PNP, β,γ-imidoadenosine 5′-triphosphate; DES, diethylstilbestrol

* Corresponding author. Fax: +4202-4712253; E-mail: kotyk@biomed.cas.cz

PII S0005-2736(97)00216-2

ing the most intriguing one of the lot [8]. It is this domain that, in response to sugar metabolism, activates the enzyme in a relatively stable way so that the H^+-ATPase can be isolated from the yeast in two different states, depending on whether, prior to disintegration, the cells were incubated for several minutes with glucose or a similar sugar, or maintained without substrate [9,10]. Studies using site-directed mutagenesis permitted to propose a model in which the ATP-binding site appears to be influenced by mutations in transmembrane helices 1 and 2 [11] and can, apparently, bind to the C-terminal regulatory domain [12], the binding being released by a glucose-dependent phosphorylation of Thr-912 assisted by a vicinal serine, as well as of Ser-899, which activates the ATPase.

It was these two different forms of the enzyme, designated here as A-ATPase and B-ATPase, that were the object of secondary structure examination. A number of H^+-ATPase inhibitors have also been tested [10,13,14], the general result being that the two ATPase forms differ quite substantially in their sensitivity and, presumably, in their secondary and/or tertiary structure. Here, we present an FT-IR spectroscopic study of secondary structure of the two enzyme forms. The use of the inhibitor DES and thermal denaturation also provided information on the tertiary structure of the two forms. A detailed analysis of the data provides support for the proposed model of glucose-dependent activation of H^+-ATPase [12].

2. Materials and methods

2.1. Materials

Deuterium oxide (99.9% D_2O), DCl and KOD were purchased from Aldrich. MES, AMP-PNP and diethylstilbestrol were purchased from Sigma. All other chemicals were commercial samples of the highest quality available.

2.2. Yeast strain and its cultivation

Saccharomyces cerevisiae K (CCY 21-4-60) was grown for 17 h at 30°C in a medium containing 2% (W/V) yeast extract (Difco) and 5.8% (W/V) glucose, adjusted to pH 4.6 with 1 M HCl. After harvesting, the yeast was washed twice with distilled water. One-half of the cells were incubated in 0.1 M glucose, the other half in 0.1 M sorbitol at 30°C for 10 min. The incubation of cells with glucose led to the activation of the H^+-ATPase [9] while the incubation with sorbitol (a nonmetabolisable sugar alcohol) did not activate the enzyme.

2.3. Cell homogenisation

The yeast cells were disrupted in a Gaulin laboratory homogeniser (Model 15M-8TA, Hilversum, The Netherlands) at 4°C, using a mixture of 1 mM $MgCl_2$, 50 mM Tris and 0.25 M glucose (pH 7.5) for cells preincubated with glucose, and 1 mM $MgCl_2$, 50 mM Tris and 0.25 M sorbitol (pH 7.5) for cells preincubated with sorbitol. Phenylmethylsulfonyl fluoride was added to 1 mM concentration to prevent protein degradation.

2.4. Isolation of plasma membranes and purification of the ATPase

Basically, the method of Goffeau and Dufour [15] was followed for the isolation and purification of plasma membranes from which the ATPase was purified by the method described by Serrano [16].

2.5. Activity and purity of the H^+-ATPase

Specific activity of the ATPase was determined according to Goffeau and Dufour [15] and found to be, on average, 3.5 μmol phosphate hydrolysed from ATP in 1 min per 1 mg protein for the activated enzyme and, on average, 0.8 μmol phosphate for the basal-level enzyme, the ratio of activities being identical with that found with purified plasma membranes, before and after activation [9,10].

The samples used for FT-IR analysis showed a single major band at M_r 100 000 in SDS-polyacrylamide gel electrophoresis – there were a maximum of 15% impurities at M_r values below 30 000.

2.6. Preparation of samples for IR measurement

Typically, 1.5 mg of enzyme were suspended in 300 μl 60 mM MES, 10 mM $MgSO_4$ buffer prepared

either in H_2O or D_2O at pH or pD of 6.1. The protein suspension was then centrifuged at 500 000 × *g* for 20 min and the pellet resuspended in 300 μl of buffer and centrifuged again. This procedure was repeated four times. For the experiments with DES or AMP-PNP, the pellet was treated in the last washing with 300 μl of buffer containing 7 mM AMP-PNP or 0.3 mM diethylstilbestrol. The inhibitor and AMP-PNP were in contact with the H^+-ATPase for 12 h at 4°C and all samples were in contact with either the H_2O or the D_2O medium for 24 h before IR analysis.

2.7. Infrared spectra

After the last centrifugation, the pellet, together with some drops of buffer used in the last washing, was collected and placed between two CaF_2 windows, separated by a 6 or 12 μm tin spacer for the experiments in H_2O and D_2O, respectively. The CaF_2 windows were then mounted in a 20 500 cell (Graseby Specac, Orpington, Kent, UK). The samples were analysed using a Perkin–Elmer 1760-x Fourier transform infrared (FT-IR) spectrometer which was continuously purged with dry air at dew point of −40°C at least 24 h before, and during spectra acquisition. Thereafter, 256 or 16 spectra, at 2 cm^{-1} resolution, were averaged for each sample at a temperature equal to or higher than 20°C, respectively. The sample temperature was controlled by an external bath circulator (Haake F3). For the thermal denaturation experiments, the temperature was raised in 5°C steps and maintained at the desired value for 6 min before spectrum acquisition. Buffer spectra were collected under the same scanning and temperature conditions as sample spectra. An interactive difference routine was used to subtract the spectrum of buffer from the spectrum of sample. Proper subtraction of H_2O was judged to yield an approximately flat baseline at 1900–1400 cm^{-1} while subtraction of D_2O was adjusted to the removal of the D_2O bending absorption near 1220 cm^{-1} [17]. A normal Beer Norton apodisation function and a deuterated triglycine sulphate detector were used in these experiments. Second-derivative spectra were calculated over a 9-data point range (9 cm^{-1}). Deconvolution parameters were set with the half-bandwidth at 18 cm^{-1} and a resolution enhancement factor of 2.5.

3. Results

3.1. Infrared spectra

The infrared spectra of A-ATPase in H_2O and D_2O are shown, as an example, in Fig. 1. The exchange of H_2O for D_2O leads to a shift of the amide I maximum from 1655.5 to 1651.9 cm^{-1}, to a marked change in the shape of amide I band and to a decrease of the amide II band intensity. These spectral modifications are due to the exchange of peptide N–H for N–D [18]. Since the amide II band intensity decrease is an indication of the extent of H/D exchange, it is clear that the H/D exchange was incomplete, reflecting inadequate accessibility of the solvent to the protein. In both ATPases the exchange amounted to roughly 60% at 20°C [18].

3.2. Secondary structure elements of yeast plasma membrane A-ATPase and B-ATPase

The deconvoluted spectra of both forms of ATPase in water, normalised at the amide I band area, display the amide I component bands, with small differences in their position and intensities, as shown in Fig. 2(A). In particular, the principal amide I component at 1658.4 cm^{-1} and a shoulder at 1653 cm^{-1} are present in the spectrum of the A-ATPase. In the

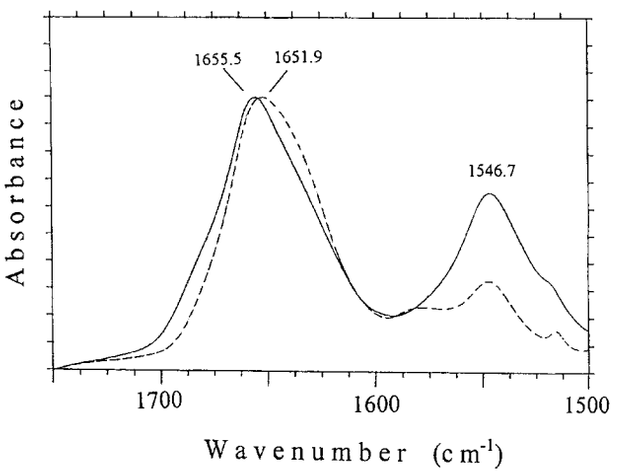

Fig. 1. Infrared spectra (1750–1500 cm^{-1} range) of A-ATPase in H_2O (continuous curve) and in D_2O (broken curve). The spectra were normalised at the amide I band height.

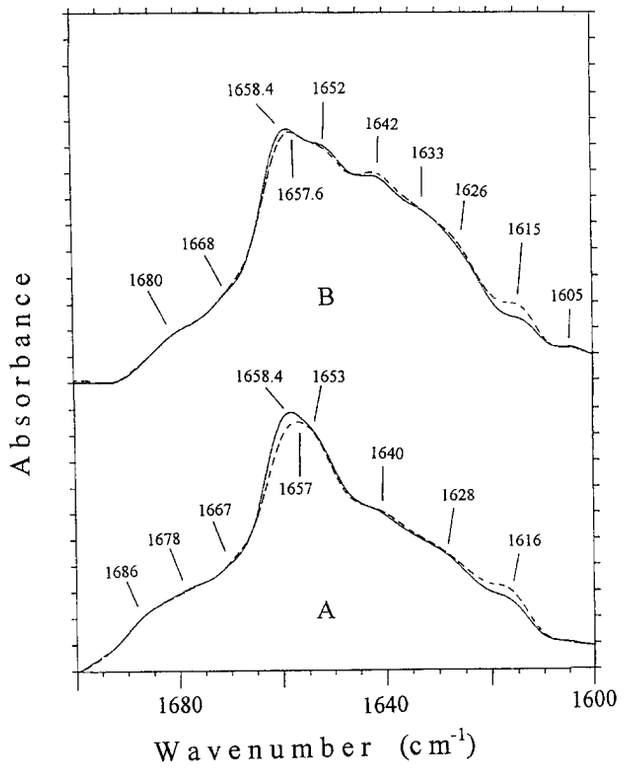

Fig. 2. Deconvoluted IR spectra (1700–1600 cm^{-1}) of A-ATPase (continuous curve) and B-ATPase (broken curve) in H_2O (part A) and in D_2O (part B). Deconvolution parameters were set with the half-bandwidth at 18 cm^{-1} and a resolution enhancement factor of 2.5.

B-ATPase spectrum the main amide I component band is seen at 1657 cm^{-1} and at a lower intensity, while the shoulder at 1653 cm^{-1} is not detectable. These bands in the spectra of proteins in H_2O reflect α-helices and random-coil conformation of the polypeptide chain that cannot be distinguished since the bands belonging to these structures are usually superimposed [19].

The overall change in shape of the amide I contour upon exposure to deuterium oxide (Fig. 1) is a consequence of the downshift in the frequency and of the decrease in intensity of some of the amide I component bands due to the exchange of peptide N–H for N–D [18]. In particular, a large shift is expected for bands belonging to turns and unordered structures, while small shifts are usually observed with bands related to α-helices and β-sheets. The deconvoluted spectra of A-ATPase and B-ATPase in D_2O display ten amide I′ bands, as shown in Fig. 2(B). The 1652, 1657.6 and 1658.4 cm^{-1} bands are characteristic of the α-helix conformation [19,20]. The position of these bands was almost the same in spectra obtained in H_2O (Fig. 2A), further supporting their assignment to α-helices. The main band is observed at 1658.4 and 1657.6 cm^{-1} in the A-ATPase and B-ATPase spectra, respectively, and, as in case of spectra obtained in H_2O, the intensity of the latter band is lower than that of the former. The two α-helix bands, observed also in other proteins [21], suggest the presence of two different populations of α-helices that could differ in the hydrogen-bonding pattern (e.g. distorted helices) and/or could be differently exposed to the solvent. They could reflect, for instance, α-helices buried in the core of the protein or in contact with lipids, and/or distorted helices, while the 1652 cm^{-1} band could be related to more regular helices and/or to more solvent-exposed α-helix segments.

The 1626 and 1633 cm^{-1} bands are characteristic of β-sheets, and the 1668 and 1642 cm^{-1} bands are due to turns and unordered structures, respectively [19,20]. However, the latter band could also be due to loops since it is seen also in the spectrum recorded in H_2O. The broad 1680 cm^{-1} band is more difficult to assign since normal-mode calculations [22] and empirical observations [20] have shown that both β-sheets and turns absorb between 1660 and 1690 cm^{-1}. The large shift of the 1686 cm^{-1} band in H_2O to 1680 cm^{-1} in D_2O (Fig. 2) suggests that turns belong to this band, but the presence of the 1678 cm^{-1} band in H_2O which is not visible in the spectrum obtained in D_2O suggests the possibility that also β-sheets could contribute to the 1680 cm^{-1} band.

The 1615 and 1605 cm^{-1} bands are outside the range of frequencies usually observed for polypeptide segments arranged in a particular secondary structure conformation and they can be assigned to amino acid side-chain absorptions [23]. The 1615 cm^{-1} band, however, could also reflect intermolecular hydrogen bonding which would, thus, be present to a larger extent in B- rather than in A-ATPase.

The small differences present in the spectra reported in Fig. 2A and 2B indicate that the two enzyme forms have a very similar secondary structure with minor differences in the content of the two populations of α-helices. The lower intensity of the 1657.6 cm^{-1} band, compared with the 1658.4 cm^{-1} peak, suggests a lower content of the particular popu-

lation of α-helices related to these bands in the B-ATPase rather than in the A-ATPase.

3.3. Effect of AMP-PNP and of DES on the secondary structure of yeast plasma membrane H^+-ATPase

The binding of the nonhydrolyzable ATP analogue AMP-PNP to the A-ATPase ATP-binding site did not modify significantly its IR spectrum, indicating that the secondary structure of the active enzyme is not affected by it (data not shown). On the other hand, when A- or B-ATPase were incubated with DES their IR spectra changed (Fig. 3). In particular, there were changes in the α-helix region (1660–1650 cm^{-1}). In the presence of DES, the two α-helix bands are less distinguishable and appear as a unique asymmetrical broad band with maximum at 1656.9 cm^{-1} in A-ATPase, and at 1655.7 cm^{-1} in B-ATPase (Fig. 3). The unique asymmetrical band can be due to a reduction in intensity of the 1658.4 or 1657.6 cm^{-1} bands and of a concomitant increase in intensity of the 1652 cm^{-1} band, as suggested by a comparison of the IR spectra of the two enzyme forms with and without the inhibitor (Fig. 3). These data indicate that the inhibitor affects the two different populations of α-helices by modifying their content ratio, most probably by inducing a higher exposure of buried helices (1658.4 cm^{-1} and 1657.6 cm^{-1} bands) to the solvent. The presence of DES also induces a marked change in the region of amino acid side-chain absorption (below 1620 cm^{-1}) in both A-ATPase and B-ATPase spectra. The original 1615 cm^{-1} band is downshifted in frequency, suggesting that, in both ATPase forms, the binding of DES modifies the interaction pattern between the amino acid side-chain moieties of the polypeptide.

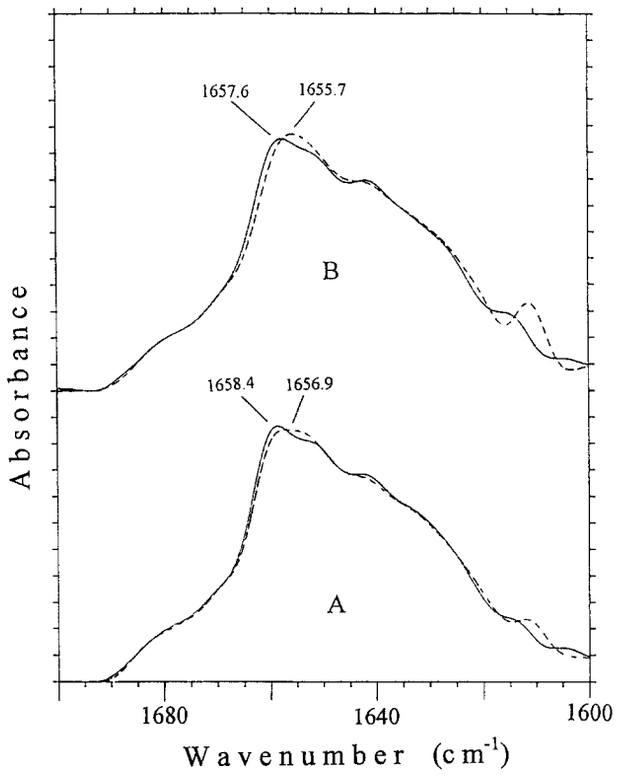

Fig. 3. IR spectra (amide I′ band) of A-ATPase (part A) and B-ATPase (part B). Control spectra are shown as a continuous line, spectra in the presence of DES as a broken line. Deconvolution as in Fig. 2.

3.4. Quantitative analysis of the secondary structure of the two ATPase forms

The secondary structure composition was obtained by curve-fitting of the original absorbance amide I′ band. Table 1 reports the results for the active and less active enzyme with and without AMP-PNP or DES. The data show small differences between the secondary structure of the two enzyme forms as previously suggested by the qualitative analysis of their IR spectra. The presence of AMP-PNP does not significantly affect the secondary structure of A-ATPase. Conversely, and in accordance with the qualitative analysis, both A- and B-ATPase in the presence of DES show a reduced content of the 1658 cm^{-1} α-helix band and an increased content of the 1652 cm^{-1} α-helix band. The curve-fitting data show also that DES induces an increase in the content of the 1633 cm^{-1} band and a decrease of the unordered structures and/or loops (1642 cm^{-1} band).

3.5. Thermal stability of the two forms of ATPase

The increase in temperature of the protein samples led to different modifications of the IR spectrum. The most evident change induced by high temperature in the 1700–1600 cm^{-1} region is the formation of two bands close to 1620 and 1680 cm^{-1}, as shown in Fig. 4 for A-ATPase. These peaks are, apparently, due to intermolecular interactions leading to aggregation of

Table 1
Calculated fractional areas (in percent) of the amide I′ component bands of A- and B-ATPase. The calculations were made on absorbance spectra recorded at 20°C. The fitting was performed using Lorentzian curves. The percentages have been rounded to the nearest integer. The amino acid side-chain absorption was not taken into account here. The symbols α, β, *r* and *t* stand for α-helix, β-sheet, random-coil and turns, respectively. The standard deviations lay within the 0.0021–0.0035

Original amide I′ component	A-ATPase	A-ATPase + AMP-PNP	A-ATPase + DES band (cm^{-1})	B-ATPase	B-ATPase + DES
1626(β)	9	10	15	10	14
1633(β)	15	15	17	15	18
1642(r/loops)	22	22	15	22	14
1652(α)	21	21	25	21	25
1658(α)	20	20	15	19	16
1668(t)	9	9	9	10	9
1680(β/t)	4	3	4	3	4

the polypeptide segments that underwent thermal denaturation [24,25]. The resolution-enhanced spectra also reveal a temperature-dependent decrease in the intensity of the β-sheet and α-helix bands, due to protein denaturation, and a temperature-dependent downshift in frequency of the α-helix band, due mainly to further H/D exchange. The temperature-dependent decrease in intensity of the residual amide II band ($1547\,cm^{-1}$) indicates a further H/D exchange due to a loosening of the enzyme structure induced by high temperature. The broad band centered at $1651\,cm^{-1}$ in the spectrum recorded at 95°C indicates that the protein retains some α-helical elements even at such a high temperature. Plots of α-helix position as a function of temperature (data not shown) revealed that the downshift in frequency starts at ca. 35–40°C, indicating that the protein begins to be more accessible to the solvent at this temperature. The spectrum of B-ATPase as a function of temperature had a similar pattern (data not shown).

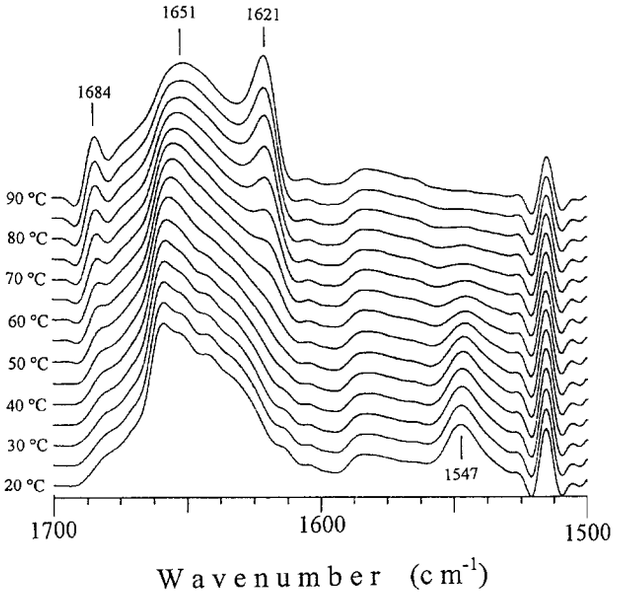

Fig. 4. Deconvoluted spectra ($1700–1500\,cm^{-1}$) of A-ATPase as a function of temperature. Spectra were collected in 5°C steps, starting from 20° to 90°C. Deconvolution as in Fig. 2.

Fig. 5 shows the thermal denaturation progress of A-ATPase and B-ATPase, under different conditions, evidenced by monitoring the width at 3/4 of the amide I′ band height as a function of temperature [26]. The temperature of maximum protein denaturation, corresponding to the curve inflection points, is higher in B-ATPase than in A-ATPase, indicating a lower thermal stability of the latter. Addition of DES lowered the thermal stability of both H^+-ATPases, while the nonhydrolysable ATP analogue AMP-PNP slightly increased the thermal stability of A-ATPase. In all cases, the onset of thermal denaturation could be observed at 55–60°C.

3.6. Difference spectra

The temperature-dependent changes in an IR spectrum can be observed in detail from the difference spectra obtained by taking the difference between two spectra recorded at adjacent temperatures [25]. The difference spectra for the A-ATPase are shown in Fig. 6. Both negative and positive peaks reflect the total changes in a particular band present in the two IR spectra to be subtracted and their characteristics

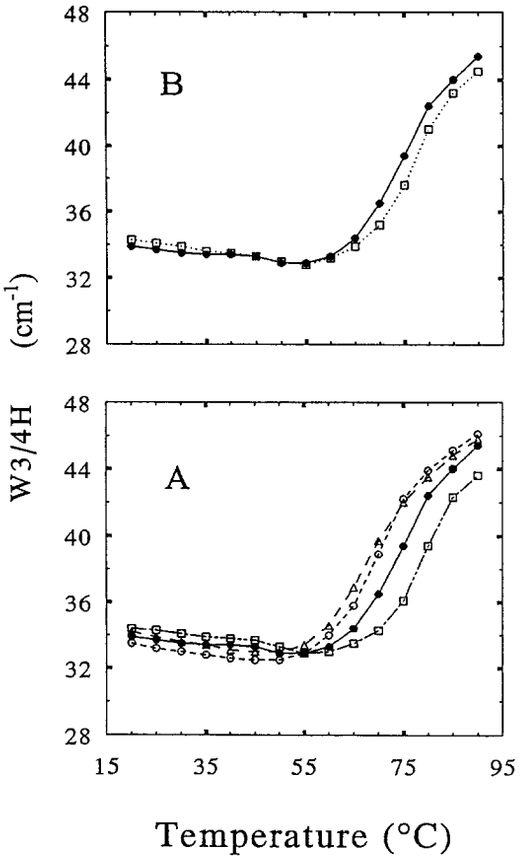

Fig. 5. Thermal denaturation of H^+-ATPase as monitored by the width at 3/4 the height of the amide I′ band. Panel A: (●) – control A-ATPase; (○) – A-ATPase with DES; (□) – control B-ATPase; and (△) – B-ATPase with DES. Panel B: (●) – control A-ATPase; (□) – A-ATPase with AMP-PNP.

depend on a number of factors [27]. Positive or negative peaks can reflect an increased or decreased intensity, respectively, of the original peaks present in the two spectra subjected to subtraction. In particular, the negative 1547 cm^{-1} band reflects a reduced residual amide II band intensity in the spectrum recorded at higher temperature and it indicates a further H/D exchange occurring in this sample. The largest negative 1547 cm^{-1} peak is seen in difference spectrum (**e**), obtained by taking the difference between spectra recorded at 55°C and 50°C, respectively. This result indicates that the largest H/D exchange took place between 50° and 55°C. This could be due to:

1. protein denaturation (loss of secondary structural elements), or
2. relaxation of the protein structure that would allow the solvent (D_2O) to reach more polypeptide segments, without remarkable protein denaturation.

Negative bands in the amide I′ region may reflect protein denaturation and/or band shifts, if positive adjacent bands of similar intensity are also present. The latter event may be represented by the negative 1662 and positive 1652 cm^{-1} bands. While the interpretation of the possible events related to these two small bands in spectra (**b–d**) is difficult, the interpretation of negative and positive bands in the spectra (**e–l**) may be more straightforward. In particular, the negative band represents mainly protein denaturation which is accompanied by protein aggregation, as revealed by the presence of the two positive bands close to 1680 and 1620 cm^{-1}. All these negative and

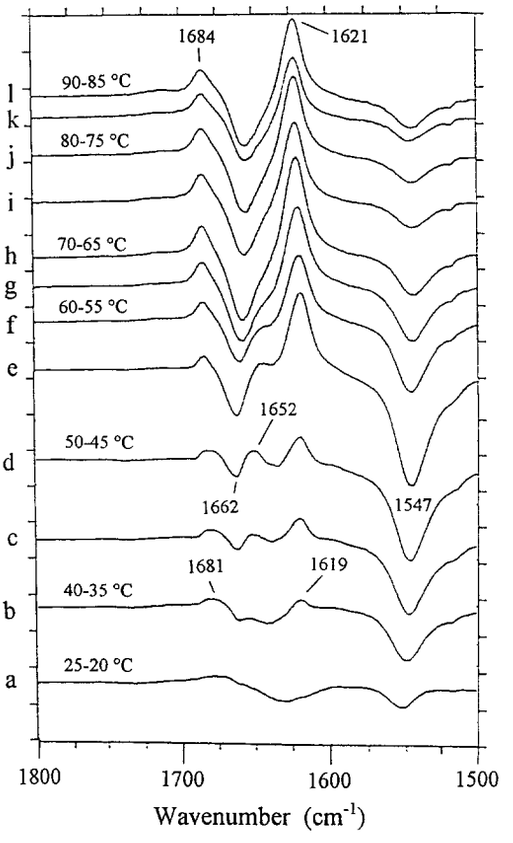

Fig. 6. Difference spectra (1800–1500 cm^{-1}) between two original absorbance spectra of A-ATPase recorded at different temperatures. Spectrum **a** was obtained by calculating the difference between the spectrum recorded at 25°C and that at 20°C (25–20°C). Similarly, spectra (**b–l**) refer to differences between those recorded at temperatures 40–35°C all the way to 90–85°C.

positive bands display their maximum intensity in spectrum (**h**) indicating that the maximum of protein denaturation and aggregation occurs at 65–70°C. So, while in spectra (**e–l**) protein denaturation occurs to a large extent, in spectra (**b–d**) protein denaturation, if present, occurs to a very small extent.

Difference spectra obtained with the B-ATPase were qualitatively almost identical.

Taken together, the data of difference spectra show that the maximum of protein denaturation (and aggregation) and the maximum of H/D exchange do not occur at the same temperature. The increase in temperature induces first a large H/D exchange that can be attributed mainly to a relaxation of the tertiary structure since none or only a partial protein denaturation is observed between 40 and 55°C. A further increase in temperature then induces a large loss of the secondary structure.

Similar difference spectra were observed for both forms of H^+-ATPase in the presence of DES (data not shown). In these spectra, however, the temperature of denaturation T_m was lower and, hence, the large H/D exchange due mainly to the loosening of the tertiary structure has, apparently, set in at a lower temperature in the presence of DES. The thermal denaturation data obtained from these difference spectra were consistent with the thermal denaturation curves shown in Fig. 5.

4. Discussion

4.1. Topology of H^+-ATPase

The yeast H^+-ATPase is a protein, the activity of which is believed to be modulated by a regulatory mechanism involving glucose-dependent phosphorylation at the C-terminus of the ATPase. Directed mutagenesis of the regulatory domain at the C-terminus [8] indicated that Arg-909 and Thr-912 are important for the regulation of ATPase activity because mutated ATPases showed reduced activation by glucose, and cells exhibited a reduced growth rate on a glucose medium. Ser-911 may also play a regulatory role, though only supportive of Thr-912. The C-terminus of yeast ATPase is believed to fold into an α-helix with Arg-909 and Thr-912 facing the same side. Thr-912 is the probable target of phosphorylation by protein kinase C which is known to activate the enzyme [28,29]. Further studies identified Ser-899 as another possible target for phosphorylation following glucose activation [12]. On the basis of these studies, it was suggested that, in the inactive state, the α-helix containing Thr-912 and Arg-909 interacts with the ATP-binding site while glucose-initiated phosphorylation of Thr-912 and/or Ser-899 would activate the enzyme by causing the C-terminus to be removed from the ATP-binding site. If this were true it would represent an analogy with the *shaker* K^+ channel [30] and the calmodulin-regulated Ca-ATPase of the plasma membrane [31], an essential site of the transport system (the neck of the channel and the ATP-binding site, respectively) being blocked in the inactive state by a segment of the polypeptide and made accessible for ATP by a conformational change. This change is caused, in the case of the Ca-ATPase, by binding of calmodulin.

Although infrared spectroscopy is a suitable technique, especially for studying the secondary structure of soluble and membrane proteins, it can also provide information on changes of the three-dimensional structure [24,25,32]. In particular, the use of DES and the combination of the thermal denaturation experiments with the analysis of difference spectra of A- and B-ATPase allowed us to present a situation that supports the proposed topological arrangement of the H^+-ATPase. Then again, this conclusion is not in agreement with the recent observation [33] that addition of glucose to yeast cells brings about a general decrease in phosphorylation, even if, apparently, at sites other than those in the regulatory C-terminal domain.

4.2. Secondary structure and effect of AMP-PNP and DES

The yeast H^+-ATPase probably contains ten transmembrane helices and several functional domains on the cytoplasmic side of the membrane [7]. The secondary structure of these domains consists of turns and loops, of β-sheets and of a number of α-helices, including the C-terminus [34]. In agreement with this, the IR data show that the H^+-ATPase apparently contains a major portion of α-helical segments, there

being two distinct populations of these present in a different environment. In particular, the 1658.4 cm^{-1} band belongs to α-helices less accessible to the solvent (included here are transmembrane helices and those buried in the protein core) while the 1652 cm^{-1} band is attributable to the more exposed ones, such as the one in the regulatory carboxyl terminus. Qualitative and quantitative analysis revealed that, both in A-ATPase and in B-ATPase, only small differences are present in the ratio between the two α-helical populations.

The fact that DES modified significantly the secondary structure of H^+-ATPase, while AMP-PNP did not, may be an indication that the inhibitor binds to a site different from that of the ATP analogue. The binding induced a significant change in the content of the two populations of α-helices and induced an increase in the β-sheet content at the expense of unordered structures (Table 1). These changes were similar in both the A- and the B-ATPase, thereby suggesting that most probably DES binds to the same site in both enzyme forms.

4.3. Thermal stability, difference spectra and tertiary structure of the two ATPase forms in the presence of DES

The thermal denaturation curves show that DES destabilises the structure of both enzyme forms and difference spectra show that DES enhances the H/D exchange at lower temperatures with respect to the control. The binding of DES to the protein, apparently, modifies the original pattern of interactions between amino acid side-chains (Fig. 3), inducing modifications in the secondary structure. These rearrangements should lead to changes in tertiary structure as suggested, in general, by the higher accessibility of the solvent to the protein (a less compact structure) and, in particular, by the increase in the content of the solvent-exposed α-helices at the expense of the buried ones (Table 1 and Fig. 3). The data thus indicate that, in addition to changes in secondary structure, DES induces a concomitant loosening of the tertiary structure of both enzyme forms.

The similarity of the thermal denaturation and H/D exchange capability of A- and B-ATPases in the presence of DES (both are downshifted in temperature with respect to the control) disappears when comparing the data of the two enzyme forms without DES. While T_m is higher in B-ATPase than in A-ATPase, the H/D exchange ability match almost perfectly (data not shown). This apparent discrepancy may be explained by the model proposed for the glucose-initiated activation of H^+-ATPase. In fact, the association of the C-terminus with the ATP-binding site would result in a more stable structure of B-ATPase than of A-ATPase, in agreement with the thermal denaturation curves. The lack of significant difference in the H/D exchangeability of the two enzyme forms may be explained by the fact that the α-helix at the C-terminus is cytoplasmic and, thus, a high H/D exchange is expected to occur there. As a consequence, the association of the α-helix with the ATP-binding site would not lead to marked differences in the H/D exchange pattern of the two enzyme forms.

The ability of DES to modify the secondary structure and to loosen the tertiary structure of both enzyme forms may also be consistent with the model that proposes an association of helices 1 and 2 with the cytoplasmic domain of ATP binding [11]. Such an association should result in a more stable structure and should keep some α-helical cytoplasmic elements away from direct contact with the aqueous milieu. Binding of DES would disrupt this association, leading to an increase of the content of solvent-exposed α-helices and to a decrease in the content of the buried ones and a concomitant loosening of the tertiary structure as described above.

4.4. Note on H / D exchange

Clearly, not all hydrogen atoms of the two ATPase forms are exchangeable for deuterium at 20°C even after multiple washings with heavy water and exposure to it for 24 h. A note is in order, here, on the inhibitory effect of heavy water in H^+-ATPase activity both in terms of acidification and in terms of ATP hydrolysis [14,35]. This is an immediate kinetic effect which apparently has to do with the double mass of D^+ compared with H^+ and consequent differences in the binding to various protonophilic sites involved in transport. It does not, however, alter the structure of the enzyme – if anything, deuterium oxide stabilises it [36,37].

Acknowledgements

The work described here was supported by grants from MURST (60%) to FT and EB, and by Grant No. 204/96/1313 of the Grant Agency of the Czech Republic to GL and to AK.

References

[1] A. Goffeau, C.W. Slayman, Biochim. Biophys. Acta 639 (1981) 197–223.
[2] A. Goffeau, N.M. Green, in: C.A. Pasternak (Ed.), Monovalent Cations in Biological Systems, CRC Press, Boca Raton, 1990, pp. 155–169.
[3] Serrano, R. (1990) in The Plant Plasma Membrane (Larsson, C., and Møller, I.M., Eds.), Springer-Verlag, Berlin, pp. 127–152
[4] R.F. Gaber, Internat. Rev. Cytol. 137A (1992) 299–353.
[5] A. Wach, A. Schlesser, A. Goffeau, J. Bioenerget. Biomembr. 24 (1992) 309–317.
[6] J.V. Møller, B. Juul, M. le Maire, Biochim. Biophys. Acta 1286 (1996) 1–51.
[7] R. Serrano, F. Portillo, Biochim. Biophys. Acta 1018 (1990) 195–199.
[8] F. Portillo, P. Eraso, R. Serrano, FEBS Lett. 287 (1991) 71–74.
[9] R. Serrano, FEBS Lett. 156 (1983) 11–14.
[10] H. Sychrová, A. Kotyk, FEBS Lett. 183 (1985) 21–24.
[11] S. Na, D.S. Perlin, D. Seto-Young, G. Wang, J.E. Haber, J. Biol. Chem. 268 (1993) 11792–11797.
[12] P. Eraso, F. Portillo, J. Biol. Chem. 269 (1994) 10393–10399.
[13] J.-P. Blanpain, M. Ronjat, P. Supply, J.-P. Dufour, A. Goffeau, Y. Dupont, J. Biol. Chem. 267 (1992) 3735–3740.
[14] A. Kotyk, M. Dvořáková, Biochim. Biophys. Acta 1104 (1992) 293–298.
[15] A. Goffeau, J.P. Dufour, Meth. Enzymol. 157 (1988) 528–533.
[16] R. Serrano, Meth. Enzymol. 157 (1988) 533–544.
[17] D.C. Lee, E. Nerzyk, D. Chapman, Biochemistry 26 (1987) 5775–5778.
[18] J.E. Baenziger, N. Méthot, J. Biol. Chem. 270 (1995) 29129–29137.
[19] J.L.R. Arrondo, A. Muga, J. Castresana, F.M. Goñi, Prog. Biophys. Mol. Biol. 59 (1993) 23–56.
[20] D.M. Byler, H. Susi, Biopolymers 25 (1986) 469–487.
[21] A. Muga, D.P. Cistola, H.H. Mantsch, Biochim. Biophys. Acta 1162 (1993) 291–296.
[22] S. Krimm, J. Bandekar, Adv. Protein Chem. 38 (1986) 181–364.
[23] Y.N. Chirgadze, O.V. Fedorov, N.P. Truskina, Biopolymers 14 (1975) 679–694.
[24] J. Skorko-Glonek, K. Krzewski, B. Lipinska, E. Bertoli, F. Tanfani, J. Biol. Chem. 270 (1995) 11140–11146.
[25] B. Banecki, M. Zylicz, E. Bertoli, F. Tanfani, J. Biol. Chem. 267 (1992) 25051–25058.
[26] G. Fernandez-Ballester, J. Castresana, J.L.R. Arrondo, J.A. Ferragut, J.M. Gonzales-Ros, Biochem. J. 288 (1992) 421–426.
[27] J. Umemura, D.G. Cameron, H.H. Mantsch, Biochim. Biophys. Acta 602 (1980) 32–44.
[28] J. Becher dos Passos, M. Vanhalewyn, R.L. Brandão, I.M. Castro, J.R. Nicoli, J.M. Thevelein, Biochim. Biophys. Acta 1136 (1992) 57–67.
[29] A. Kotyk, G. Georghiou, Cell Biol. Internat. 18 (1994) 813–817.
[30] C. Miller, Science 252 (1991) 1092–1096.
[31] E. Carafoli, J. Biol. Chem. 267 (1992) 2115–2118.
[32] C. Fini, E. Bertoli, G. Albertini, A. Florifi, F. Tanfani, Biochim. Biophys. Acta 1118 (1992) 187–193.
[33] E. Estrada, P. Agostinis, J.R. Vandenheede, J. Goris, W. Merlevede, J. François, A. Goffeau, M. Ghislain, J. Biol. Chem. 271 (1996) 32064–32072.
[34] V.V. Petrov, C.W. Slayman, J. Biol. Chem. 270 (1995) 28535–28540.
[35] A. Kotyk, M. Dvořáková, J. Koryta, FEBS Lett. 264 (1990) 203–205.
[36] M. Tuena de Gómez Puyou, A. Gómez-Puyou, J. Cerbón, Arch. Biochem. Biophys. 186 (1978) 72–77.
[37] L.P. Ma, R.L. Magin, G. Bacic, F. Dunn, Biochim. Biophys. Acta 978 (1989) 283–292.